MEASUREMENT AND INTERPRETATION OF NON-ARCHIE RESISTIVITY BEHAVIOR IN MODEL AND REAL VUGGY CARBONATES

G.S. Padhy, M.A. Ioannidis, C. Lemaire, M. Coniglio
University of Waterloo, Waterloo, Canada

This paper was prepared for presentation at the International Symposium of the Society of Core Analysts held in Trondheim, Norway 12-16 September, 2006

ABSTRACT

Carbonates are unique because of intrabasinal origin, primary dependence on organic activities and susceptibility to modification by post-depositional mechanisms. The diverse post-depositional diagenetic processes give rise to complex pore microstructures and porosity at multiple scales in vuggy carbonates. Pores in vuggy carbonates can range from less than a micron (matrix pores) to several millimeters (vugs) and different pore populations (micropores, mesopores and vugs) may or may not form percolating networks. Such structural complexity typically results in a relationship between water saturation and resistivity index that deviates significantly from the classical Archie behavior that is common for clastic rocks. Non-Archie behavior has been qualitatively explained by theoretical models, based on simple mixing laws [5, 6] or effective medium approximation (EMA) [7], but these models have received limited validation against experimental data. To better understand this non-Archie behavior we carry out electrical resisitivity index measurements during drainage on a suite of vuggy dolomite rocks and synthetic vuggy porous media of controlled microstructure. The later are created by mixing monodispersed glass beads and much larger calcium carbonate particles in known proportions, consolidating the mixture in an oven and then dissolving the carbonate particles by flowing acid. An *in-house* built four-electrode resistivity cell is employed to measure the electrical resistivity at ambient conditions using a continuous injection method. Non-Archie behavior is observed in samples containing significant amounts of vuggy porosity. Novel measurements of the matrix and vuggy porosity and pore size distribution by a combination of DDIF-NMR and 3D single-point magnetic resonance imaging [4], in combination with drainage capillary pressure measurements by MIP, provides information on the amount and accessibility of different pore populations. A theoretical resistivity index model based on interconnectedness of two main pore populations (matrix and vug) of vuggy carbonates is quantitatively tested against the experimental resistivity index measurements during drainage. It is concluded that a more robust model is required to predict the non-Archie behavior of these vuggy carbonates.

INTRODUCTION

Recent studies have focused on modeling the capillary, flow and electrical properties of vuggy carbonates using pore network models [1, 2]. These studies have sought to account for the effect of the microstructure at two different scales, corresponding to vug and matrix pores, but validation of their results has been hampered by the lack of experimental data on systems with well characterized matrix and vuggy porosity. Insights into pore geometry and pore scale physics are essential to explain the fluid displacement characteristics. Cementation factor and saturation exponent vary widely in carbonates due to their intricate pore geometry, giving rise to complex resistivity index (RI) curves and cannot be described by a simple Archie law [9]. Many challenges still exist in understanding and predicting electrical resistivity of vuggy carbonates based on their dual pore microstructures. Proper m and n values should be used to calibrate borehole logs in order to avoid over or under estimation of water saturation. The influence of microporosity on saturation exponent was studied by Dixon and Marek [8] through laboratory investigation and was theoretically explained with simple mixing laws [5, 6] and effective medium approximation [7]. Based on these theories a mathematical model for vuggy carbonate system was tested against the experimental resistivity data.

THEORY

With the aim to test the theoretical models [5, 6, 7], we modified the general equation of Petricola and Watfa [5] based on the facts that (i) the rocks under study are water-wet, (ii) the pores always contain a layer of water along the pore boundaries and (iii) two distinct pore populations exist (vuggy and matrix pores).

For a water-wet case, the total conductivity (C) of the system is expressed as:

$$C = C_v + C_m = C_w\left(\phi_v^{m_v/X} S_{wv}^{n_v/X} + \phi_m^{m_m/X} S_{wm}^{n_m/X}\right)^X \quad (1)$$

where C_v, C_m and C_w are the conductivities of vug network, matrix network and water respectively, S_w, m and n are the saturation, cementation factor and saturation exponent respectively (with subscripts 'v' for vug pore system and 'm' for matrix pore system), ϕ_v is the vug porosity and ϕ_m is the matrix porosity. X = 1 if the two pore systems are completely parallel or X= 2 if the conductivity is through volume summation.

Average saturation S_w is related to S_{wv} and S_{wm} as [6]:

$$S_w = f_v S_{wv} + f_m S_{wm}, \text{ where } f_v + f_m = 1 \quad (2)$$

where f_v and f_m are the pore volume fractions of vug and matrix pore populations. Generally the non wetting phase invades the matrix pores at a pressure higher than that required to invade the vugs, so that S_c is the average saturation corresponding to this pressure, determined from MIP. Now, S_{wv} and S_{wm} can be expressed in terms of S_w as:

$$S_{wv} = \frac{S_w - f_m S_{wm}}{f_v}, S_{wm} = 1, \text{ for } S_w \geq S_c \quad (3)$$

$$S_{wm} = \frac{S_w}{S_c}, \text{ for } S_w \leq S_c \quad (4)$$

The matrix porosity ϕ_m is calculated from total porosity (ϕ) and vug porosity (ϕ_v) using the relation:

$$\phi_v = \frac{\phi - \phi_m}{1 - \phi_m} \quad (5)$$

All parameters of the model except cementation factor and saturation exponent are obtained from independent experiments as explained below.

EXPERIMENTAL PROCEDURE

Sample Description:
Electrical resisitivity measurements were performed on five vuggy core plugs exhibiting two distinct pore populations (matrix pores and vugs) and a non-vuggy core plug. All core plugs were 3.8 cm in diameter and about 5 cm in length. The real vuggy carbonates (13P20H, 16BP17H and 16BP8H) are Middle Silurian dolomites from Southwestern Ontario, Canada (see Table 1). The synthetic samples were made using a previously described procedure [3]. These media exhibit different amounts of vuggy porosity (SC16a and SC4b), generated by the dissolution of calcium carbonate particles of known size d_{CaCO_3} (see Table 1). Matrix porosity corresponds to the space between sintered glass beads of uniform size. Matrix pores vary in size depending on the choice of glass bead size (d_{GB}) and the extent of consolidation. The synthetic non-vuggy sample (SC6a) was made without any calcium carbonate particles resulting in a core plug containing matrix porosity only. Typical images of the pore space of each sample are shown in Figure 1. These images are small parts of high-resolution (1.87 μm/pixel) images of *entire* thin sections (2.6 cm wide) through each sample.

Sample	d_{GB} (μm)	d_{CaCO_3} (mm)	ϕ_{total} (%)	ϕ_{vug} (%)	k (mD)	m	l_c (μm)
SC16a	63-75	0.84-1.18	31.9	25.2	2406	2.68	209
SC6a	125-150	-	16.2	0	1040	1.70	57
SC4b	125-150	1.18-2.38	46.8	12.4	4740	1.47	107
13P20H	-	-	15.5	-	115	1.89	81
16BP17H	-	-	14.4	-	72	2.03	164
16BP8H	-	-	14.3	-	40	1.99	35

Table 1: Petrophysical properties of real and synthetic vuggy samples (whole core values). Total and vug porosities determined gravimetrically. Characteristic pore diameter $\ell_c = 4\sigma\cos\theta / P_c^o$ calculated from breakthrough capillary pressure measured using low-rate gas injection.

Regarding the synthetic media, Figure 1 shows matrix porosity inhomogeneity in the most consolidated sample (SC16a) and the presence of *matrix* pores of size greater than the size of individual glass beads (SC6a and SC4b), corresponding to packing "flaws". The pore space of real vuggy carbonate samples has a *self-similar* appearance. Both touching and isolated vugs are apparent in the real and synthetic media.

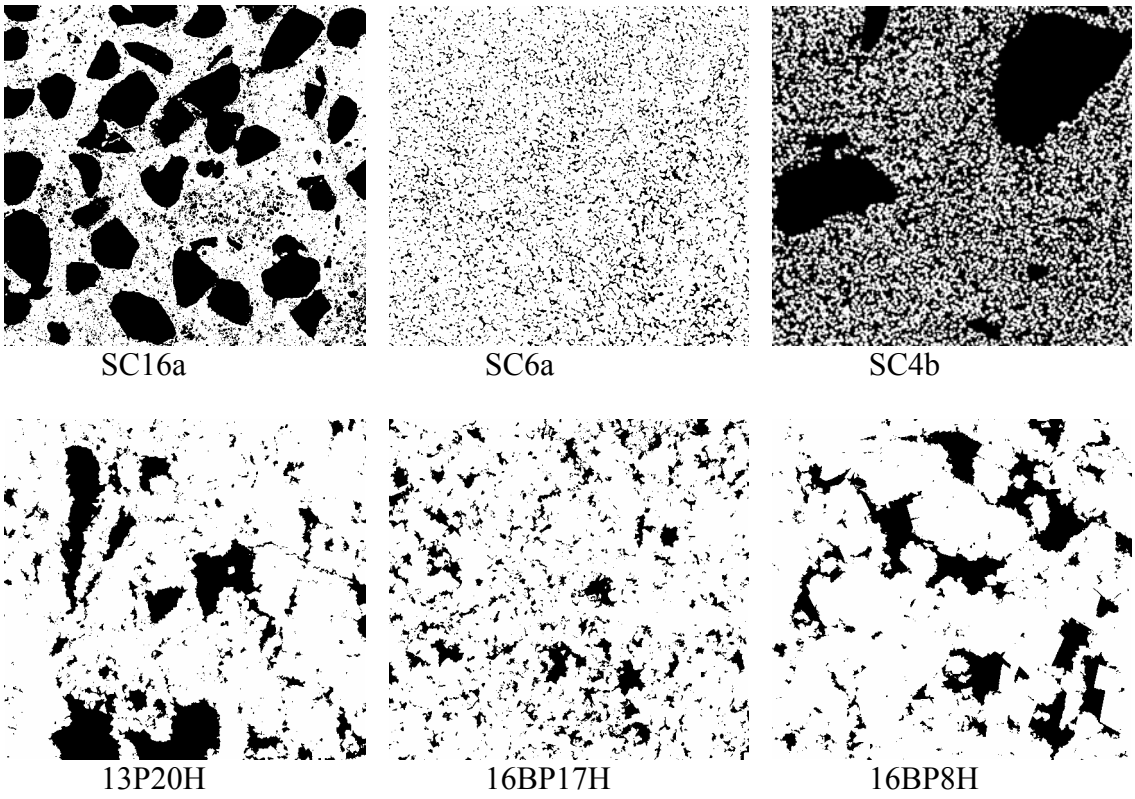

Figure 1: Representative images (cropped from images of entire thin sections) of the pore space in real and synthetic vuggy porous media. Each image represents an area of 9.2 mm x *9.8 mm.*

Equipment Setup:

The *in-house* designed four-electrode system used to measure electrical resisitivity is shown in Figure 2. The current electrodes are made by soldering a shielded copper wire to a steel wire screen. The wire screen provides a cross-sectional contact with the sample and better fluid distribution at the injection face. The wire is passed through the end stems. A Teflon disk is used to isolate the screen from the flood head. The potential electrodes (buttons) are made up of brass and are mounted 1-cm apart from each other on the rubber sleeve. Shielded copper wires are soldered to the buttons and taken out of the core holder through a high pressure (up to 10,000 psi) sealing cable gland. The brass buttons are pressed against micro porous silver membrane strips ($1/8^{th}$ inch width and 1 inch length) affixed to the sample through conductive epoxy. These not only provide better contact with the sample but also cover a major portion of the sample circumference. A high precision LCR meter (QuadTech), capable of measuring

impedance/resistance from 0.00001 mΩ to 99.999 MΩ in the frequency range of 20 Hz to 1 MHz is used for all electrical measurement. Constant rate injection was done using a high pressure syringe pump (ISCO) and inlet pressure of the injected gas was monitored using a pressure transducer. The average brine saturation was determined gravimetrically using a high precision analytical balance (Denver instruments).

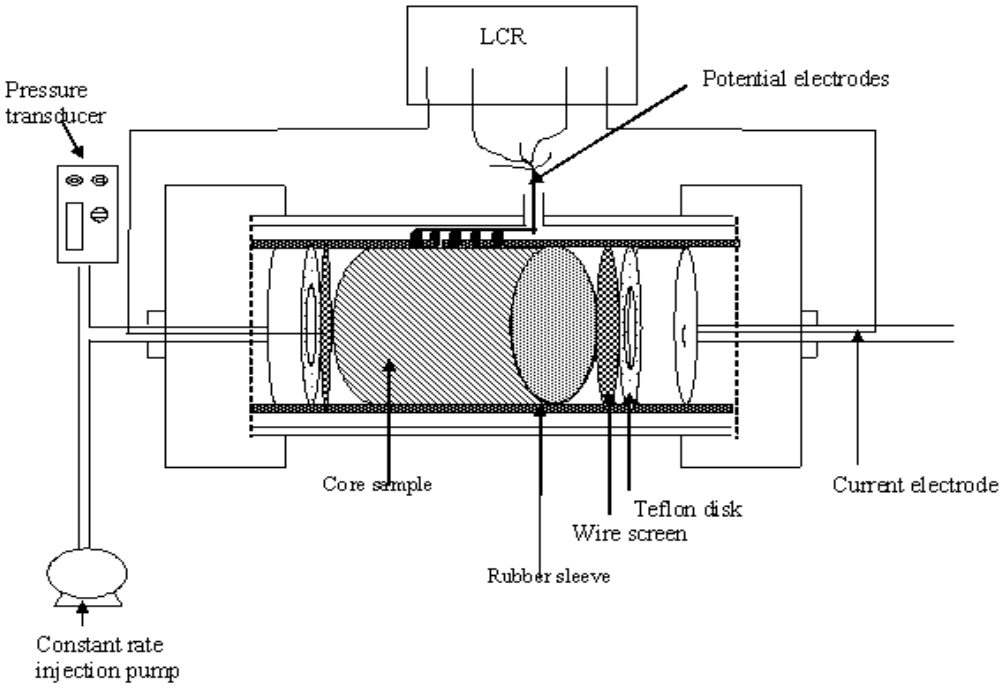

Figure 2: Schematic design of the experimental setup for electrical measurement.

RI Measurement:

The samples were saturated under vacuum and pressure using 30,000 ppm NaCl solution and placed in a sleeve equipped with a 0.2 μm hydrophilic nylon membrane at the exit face to prevent early exit of the injected non-wetting phase. The core holder was placed vertically and pressurized to 400 psi to ensure good sealing between the sample and sleeve. The sample under ambient pressure and room temperature condition was desaturated by continuously injecting humidified air at a constant rate of 0.033cc/min. The rate was chosen such that quasi-static displacement takes place. This rate is similar to the one used by Smith et al. [11] and found to be adequate for rocks with breakthrough capillary pressure lower than 8 psi. All of our samples meet this condition. The chosen injection rate represents a compromise between the need to obtain accurate results and the need to perform the test in a reasonable amount of timeThe average brine saturation was determined continuously by a gravimetric method. Electrical resistance was measured using an AC voltage of 1V at a frequency of 30 kHz. A pressure transducer was attached at the inlet to monitor the pressure of injected gas and ensure that the non-wetting phase had not exited the system. Inlet pressure, brine production and resistance data were acquired simultaneously at fixed time intervals by automated data acquisition

system. Mass balance calculation was done using the inlet pressure and rate of injection to ensure consistency between measured injection pressure and mass of brine produced.

Accuracy Check:
To check the reliability and accuracy of measurement of the *in-house* designed system Berea sandstone was first measured and the RI vs. S_w plot is shown in Figure 3. Cementation factor and saturation exponent calculated using standard Archie equations [9] were found to be in good agreement with literature values (see Table 2).

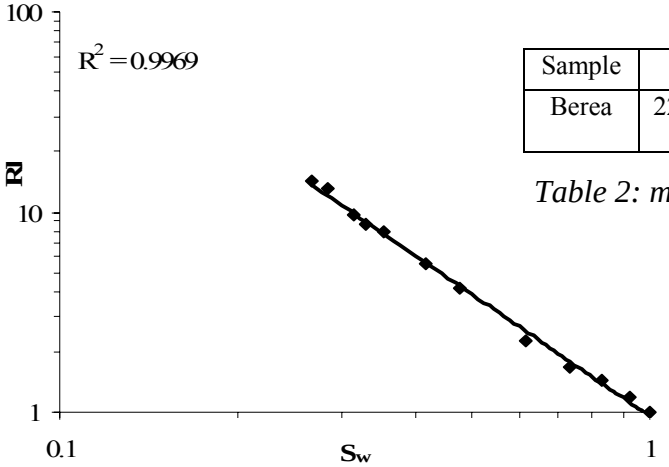

Figure 3: Resistivity Index plot of Berea sandstone

Sample	ϕ	m	n	K (mD)
Berea	22.3	1.95	2.02 (+/- 0.04)	660

Table 2: m and n values of Berea sandstone

MIP Measurement:
Mercury porosimetry tests were performed on cylindrical samples 1-cm in diameter and 2-cm long using the PoreMaster60 (Quantachrome Instruments). The samples were analyzed in two stages, namely low pressure (<1psi to 50psi) and high pressure (20psi to 60000psi) for intrusion and extrusion.

RESULTS AND DISCUSSION

RI Measurement of Vuggy Samples:
Following the accuracy test, RI measurements during drainage are done for all the samples under consideration. Tests were repeated to ascertain reproducibility. Figure 4 shows RI plots for 3 vuggy samples (SC16a, 13P20H and 16BP8H), and plots for all other samples are shown in a later section. For all samples, a clear non-Archie behavior is observed due to the presence of bimodal pore microstructure [4]. For sample SC16a a jump at the beginning is observed possibly due to the presence of large amount of surface vugs that drained at the early stage of the experiment. A flattening out of the RI with decreasing water saturation is observed at the lowest levels of water saturation, where resistivity is dominated by thin water layers connecting pendular rings and thus becomes insensitive to saturation changes. Cementation factor (m) values for all samples are presented in Table 1. Sample SC16a shows a relatively high value of m =2.68, indicating the presence of voids which contribute a lot to porosity but little to conductivity (e.g.

poorly connected vugs [10]). Also shown in Figure 4 are plots of mass balance checks (the figures on the right hand side) for SC16a, 13P20H and 16BP8H ensuring consistency between the measured injection pressure and the injection pressure calculated from a mass balance. This calculation was based on the ideal gas law and known mass of brine produced, rate of gas injection and initial gas volume.

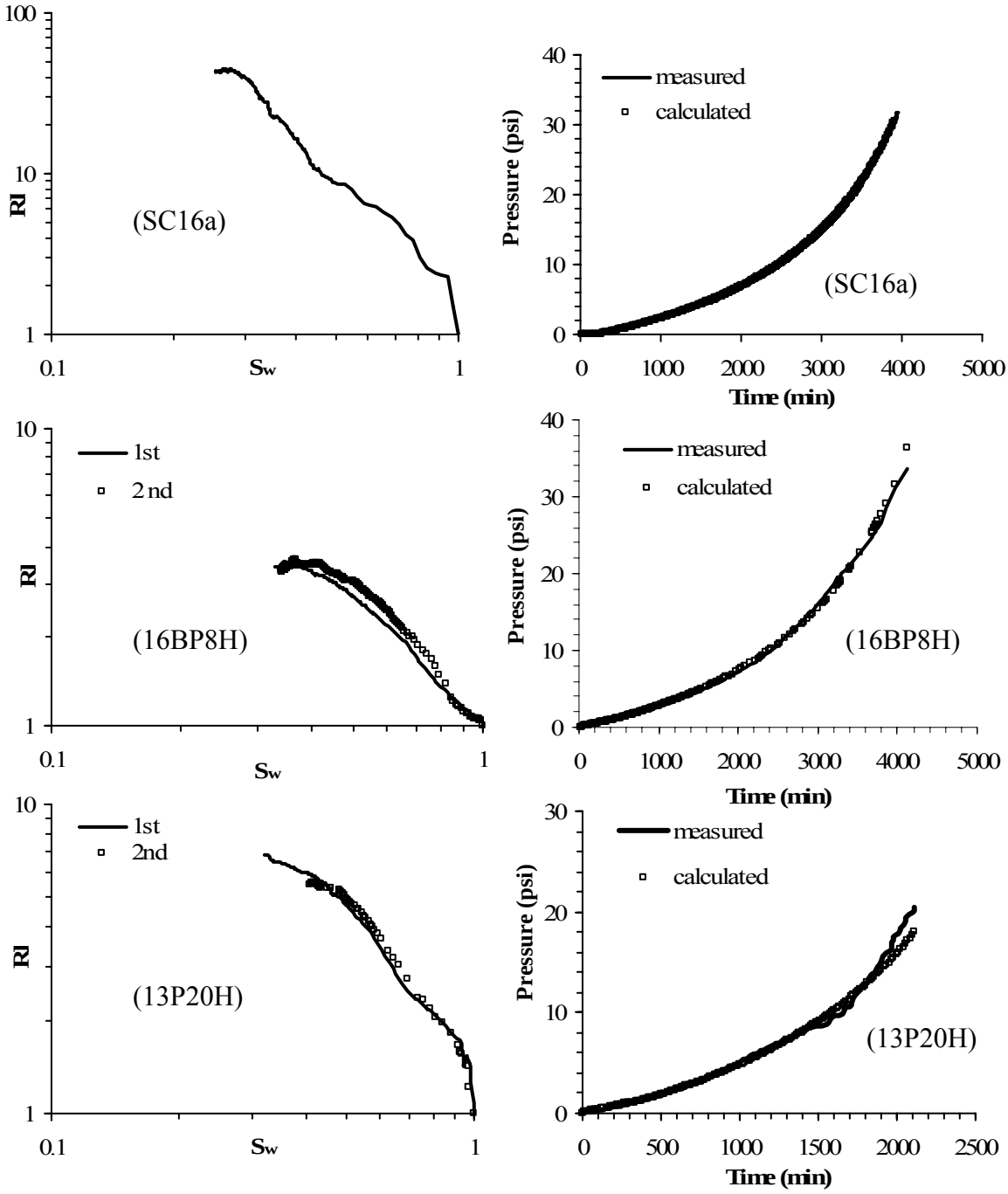

Figure 4: Resistivity Index (left) and Mass balance check (right) plots.

Comparison of MIP to Dynamic Capillary Pressure:
The inlet pressure during RI measurement was continuously recorded and plotted against saturation values to obtain the dynamic capillary pressure curves for the air-brine system. The results were in good agreement with the breakthrough capillary pressures (P_c^o) measured on the same samples under same measurement conditions. Characteristic pore diameter ($\ell_c = 4\sigma\cos\theta / P_c^o$) calculated from these breakthrough capillary pressures are shown in Table 1. Comparison of the dynamic capillary pressure and MIP data (after scaling of the former using γ_{wa} = 0.070N/m, γ_{ma} = 0.485N/m, θ_{wa} = 0° and θ_{ma} = 150°) revealed differences in capillary pressure and saturation values (Figure 5). This difference was attributed to sample heterogeneity, trapping of brine and difference in sample volume under consideration (i.e. whole plug in air-water case vs. a small piece in MIP case).

Comparison of Experimental RI to Model Predicted RI:
Figure 6 illustrates the RI measurements obtained from experiment to that predicted from the model. Reasonable agreement is observed but not perfect agreement. Out of all model parameters, S_c is determined from MIP, X is fixed at 1.5, (i.e. the total conductivity of the system is neither due to two completely parallel networks nor due to complete volume summation), ϕ_v and f_v are determined from 3D MRI/DDIF-NMR measurements [4]. The matrix porosity ϕ_m is calculated using ϕ_{total} from Table 1 and Eq. (5). f_m is determined from the relation $f_v + f_m = 1$, whereas the parameters m_v, m_m, n_v and n_m are adjustable and are determined by non-linear regression. First, the values of m_v and m_m are optimized to match the formation factors and then n_v and n_m to match the RI curves. The model parameter values for all samples are given in Table 3. The model fit is good in case of SC6a and SC4b where the pore size distribution is not complex, but it fails to deal with more complex pore microstructures [4]. Also, it was not possible to capture the flattening of RI at lower saturations.

Sample	ϕ_v (%)	ϕ_m (%)	S_c (%)	f_v	f_m	m_v	m_m	n_v	n_m	x
SC16a	25.0	9.3	50.0	0.65	0.35	2.5	2.2	4	2.88	1.5
SC6a	0	16.2	-	0	1	-	1.70	-	2.34	1.5
SC4b	12.4	39.3	100	0.3	0.7	1.83	1.48	1	1.27	1.5
13P20H	11.5	4.5	70.0	0.6	0.4	1.91	1.68	2.72	1	1.5
16BP17H	8.4	6.6	70.0	0.6	0.4	1.92	1.93	1.99	1.05	1.5
16BP8H	11.2	3.5	70	0.65	0.35	1.89	2.01	1.2	1	1.5

Table 3: Model parameters

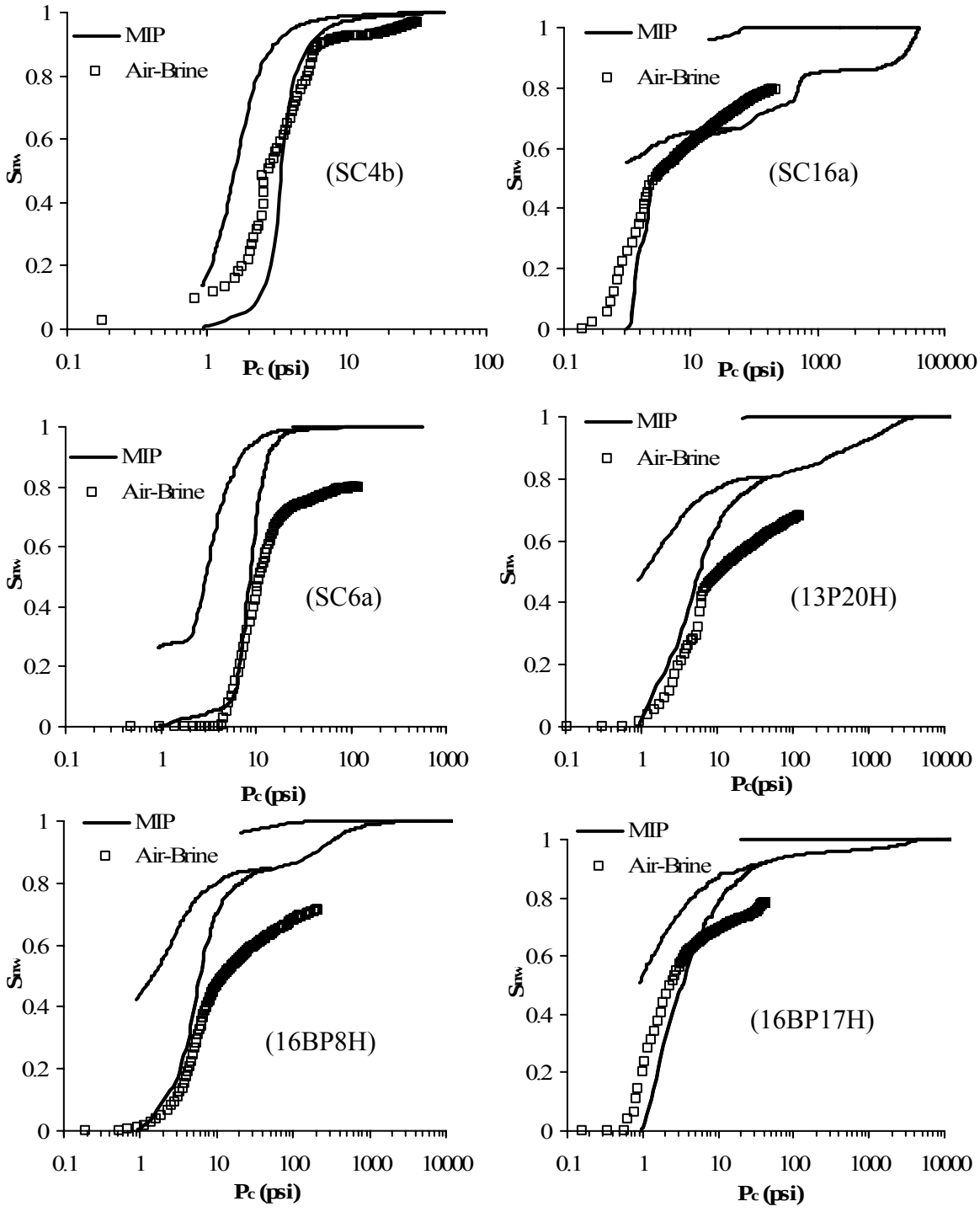

Figure 5: Comparison of air-brine and MIP capillary pressure data.

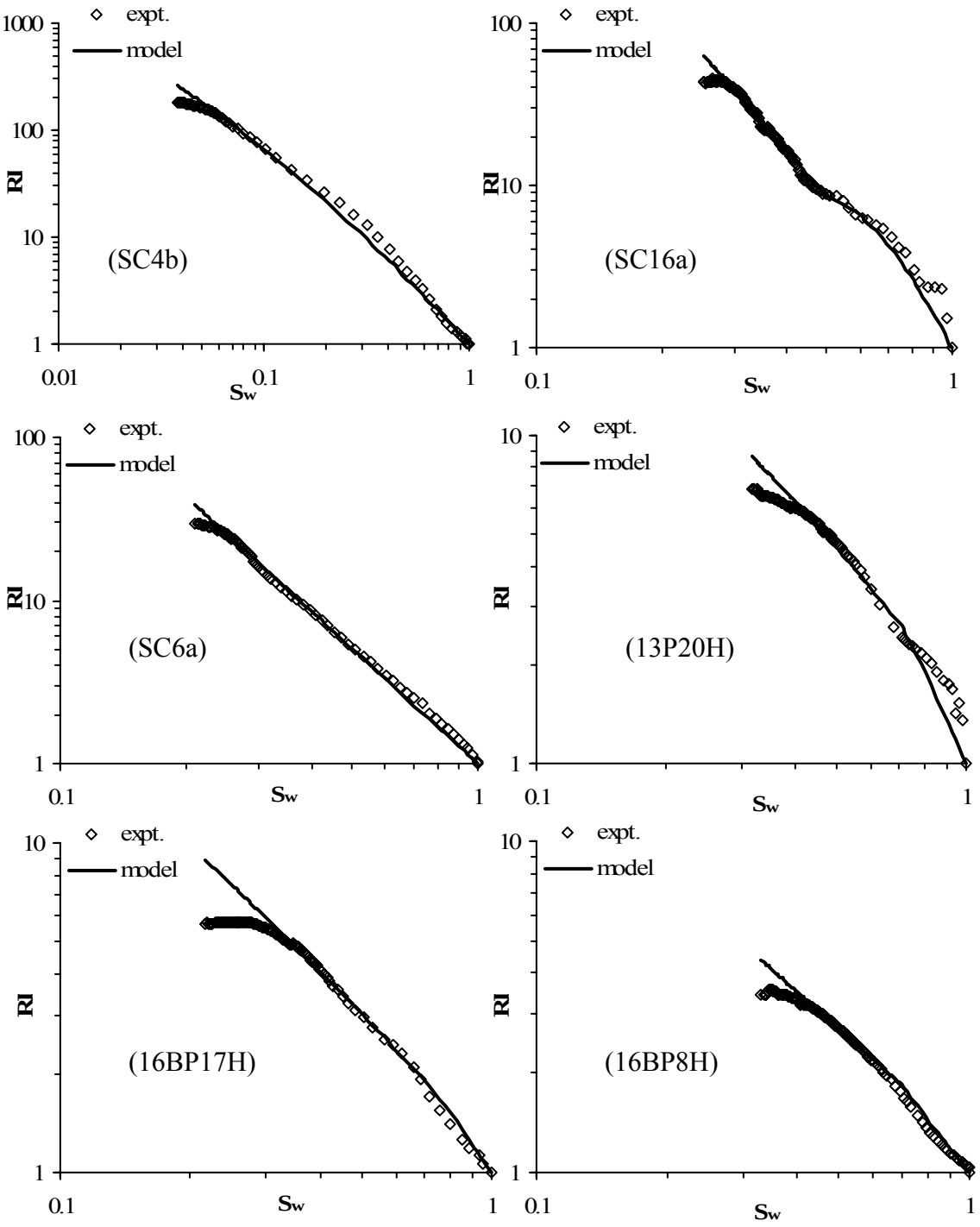

Figure 6: Comparison of RI measurements: Experiment vs. Model.

CONCLUSIONS

- The non-Archie behavior of the vuggy carbonates was solely due to pore structure effects.
- Pore size distributions obtained from DDIF-NMR/image analysis and quantification of vugs from 3D MRI helped in understanding the non-Archie behavior.
- Independent measurement of vug porosity and volume fractions of different pore populations helped in testing the validity of the theoretical model against experimental data.
- As observed, the model qualitatively explained the non-Archie behavior, but a more robust model incorporating the RI behavior at lower saturations is required for complete prediction of the RI curve for vuggy carbonates.
- Use of micro-CT characterization data in the model might help to formulate a better model.

REFERENCES

1. Ioannidis, M.A. and Chatzis, I. (2000): "A Dual-Network Model of Pore Structure for Vuggy Carbonates", *Proceedings of the Annual Symposium of the Society of Core Analysts*, SCA2000-09 , Abu-Dhabi, U.A.E.
2. Moctezuma, A., Bekri, S., Laroche, C. and Vizika, O. (2003), "A Dual-Network Model for Relative Permeability of Bimodal Rocks: Application in a Vuggy Carbonate. *Proceedings of the Annual Symposium of the Society of Core Analysts*, SCA2003-94, Pau, France.
3. Padhy, G., Ioannidis, M. A. and Lemaire, C. (2005): "Special Core analysis studies in Vuggy porous media of controlled microstructure", *Proceedings of the Annual Symposium of the Society of Core Analysts,* SCA2005-76, Toronto, Canada.
4. Padhy, G., Lemaire, C. and Ioannidis, M. A. (2006): "Mgnetic Resonance Methods for the Characterization of the Pore Space in vuggy Carbonates", *Proceedings of the Annual Symposium of the Society of Core Analysts,* SCA2006, Toronto, Canada.
5. Petricola, M.J.C. and Watfa, M. (1995): "Effect of Microporosity in Carbonates: Introduction of a Versatile Saturation Equation", *SPE Middle Eastern Oil Show,* SPE 28841, 607-615, Bahrain.
6. Fleury, M. (2002): "Resistivity in Carbonates: New Insights", *Proceedings of the Annual Symposium of the Society of Core Analysts,* SCA2002-28, Montery, USA.
7. Sen, P.N. (1997): "Resistivity of Partially Saturated Carbonate Rocks with Microporosity", *Geophysics*, **62** (2), 415-425.
8. Dixon, J.R. and Marek, B.F. (1990): "The effect of Bimodal Pore Size Distribution on Electrical Properties of Some Middle Eastern Limestones", 65th *SPE Annual technical conference and exhibition,* SPE 20601, 743-750, New Orleans, USA.
9. Archie, G.E. (1942): "The Electrical Resistivity Log as an aid in Determining some Reservoir Characteristics", Trans., AIMME, **146**, 54-67.
10. Focke, J.W. and Munn, D. (1987): "Cementation Exponents in Middle Eastern Carbonate Reservoirs", SPE FE, SPE 13735, 155-167.
11. Smith, J.D., Chatzis, I., Ioannidis, M.A. (2005): "A New Technique to Measure Breakthrough Capillary Pressure", JCPT, **44 (**11), 25 -31.